RSC Advances

ROYAL SOCIETY OF CHEMISTRY

www.rsc.org/advances

RSC Advances

PAPER

Cobalt Oxide Nanoparticles on TiO_2 Nanorod/FTO as a Photoanode with Enhanced Visible Light Sensitization

Vivek Ramakrishnan,[a] Hyun Kim,[a] Jucheol Park,[b] and Beelyong Yang*[a]

Received
Accepted

DOI: 10.1039/x0xx00000x

www.rsc.org/

Cobalt oxide nanoparticles were sensitized on hydrothermally grown TiO_2 nanorod on FTO (Fluorine-doped Tin Oxide) by eletrochemical deposition followed by rapid thermal annealing under air and N_2. We investigated the formation of nanostructure with different electrodeposition time, electrolyte concentration, and annealing temperaturefor improved photoelectrochemical (PEC) properties. Structural investigation showed the formation of mixture of CoO/Co_3O_4 oxides depending on annealing temperatures and ambients. The equilibrium of oxide formation shifted from Co_3O_4 to mixture of CoO/Co_3O_4 and finally to monoxide when temperature is lowered from 700^0C to 350^0C. Improved PEC properties were shown by mixture of oxides than system with CoO and Co_3O_4 alone on TiO_2. Electrodeposition time was found to have a linear relationship with nanoparticle size of Cobalt oxide formed on TiO_2. Here we propose a cost effective and simple method to fabricate a hetero-junction system with improved PEC properties.

Introduction

There is a growing demand for sustainable energy production using clean resources. Sunlight is the ultimate energy resource which we will able to depend on. In recent years artificial photosynthesis had become a hot topic where researchers focussing on ton to produce renewable clean energy by photocatalytic water splitting.[1-3] There are numerous ways to achieve such type of systems with main emphasis is to have highest efficiency with low cost of production and utilization of high earth abundant raw materials which include organic, inorganic and hybrid systems.

In recent years, there are many reports on efficient semiconductor based photocatalysts.[4-8] One of the methods includes preparation of nanostructures involving more than one type of semiconductor system. A tandem nanostructure consisting of n-type and p-type semiconductors for overall water splitting is always desirable without external bias.[9] Such type of multi-junction photoelectrode for overall water splitting is always challenging on the basis of electronic and thermodynamic requirements.[10-15] Titanium dioxide (TiO_2) based nanostructures have been well studied in the field of photocatalysts. It is preferred because of its chemical stability, low cost, abundance and favourable band edge alignment with water redox potentials which make them a potential candidate as photoanodes for water oxidation.[16-21]

Cobalt oxide systems (Co_3O_4 and CoO) are well studied in the field of photocatalysis. They have got wide variety of applications as well. Such as heterogeneous catalysis, Li-ion batteries, photocatalysis, solar absorbers and so on. Among which Co_3O_4 has got more prominence because of its high chemical stability. Co_3O_4 unit cell is having a spinal structure and it has got a direct optical band gap of ~1.5 – 2 eV in bulk state. But the nanoparticles of Co_3O_4 reported to have a much larger band gap (~2.5 eV) with the top level of the valence band and the bottom level of the conduction band to be 2.52 V and 0.09 V, respectively, relative to the normal hydrogen electrode (NHE). Compared to that CoO systems are not much studied widely because of its less stability and difficulty in selective preparation.[22-29] Coupling of CoO with TiO_2 with specific nanostructures could be a suitable system for overall water splitting. The bottleneck in preparing such type of nanostructure lies in the selective oxidation of Cobalt as it has three types of oxide forms which is very sensitive to the formation conditions.[30] (1) Co_3O_4, which has a spinel (a = 8.108Å) structure with a band gap of 2.07 eV. (2) Co_2O_3, Unit cell has a

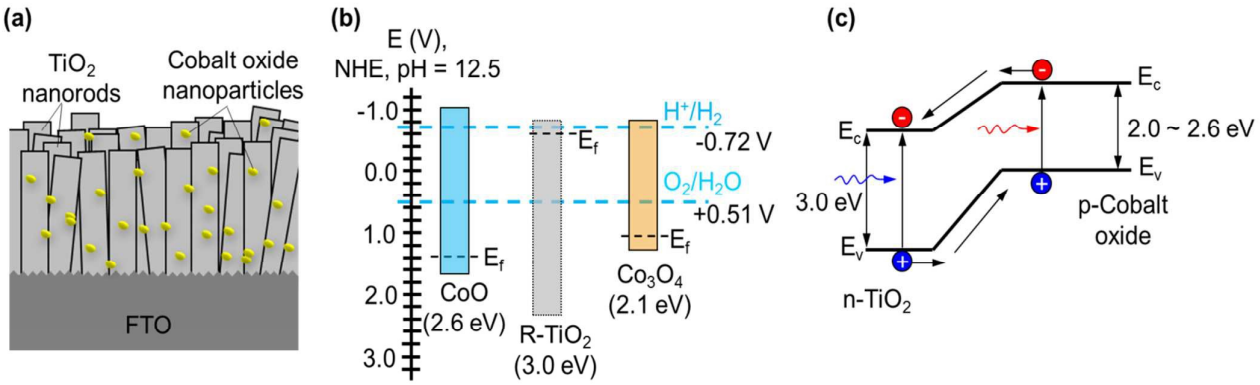

Figure 1. Schematic diagram of heterojunction system of Cobalt oxide/TiO_2 nanostructure (2) Fermi level alignment of hetero-junction system of Cobalt oxide/TiO_2 (c) electron-hole movement after hetero-junction formation.

hexagonal structure (a=4.64 Å, c=5.750 Å) with no photocatalytic activity reported best to our knowledge. (3) CoO is face centred cubic (a=4.22) with both bulk and nanoparticles reported to have a band gap of 2.6 eV. There were some attempts already carried out in preparing all nanoparticle systems of Cobalt oxide (CoO_x) and TiO_2 by sol-gel method,[26] CoO flakes spread over TiO_2 nanotube by cathodic deposition,[27] and Co_3O_4/TiO_2 by photodeposition for photocatalytic applications.[31] We prepared a system with specific nanostructure, nanoparticles of Cobalt oxides uniformly anchored even on a dense substrate, selective form of oxide utilising simple and cost effective instrumentation.

Our group have been actively studying on nanostructured semiconductor systems for photocatalytic applications.[32-35] In this work, we have systematically investigated the preparation, microstructure, selective oxide formation, and photoelectrochemical property of hetero-junction of Cobalt oxide/TiO_2 system. By two-step process, Cobalt oxide nanoparticles were engineered on TiO_2 nanorods which subsequently showed improvement in visible light sensitization attributed to the band gap of CoO and Co_3O_4.

Experimental

Preparation of TiO_2 Nanorod on FTO

TiO_2 nanorods were vertically grown by hydrothermal synthesis on FTO glass substrates (2 x2 cm) which were ultrasonically cleaned for 15 min with trichloroethylene, acetone, methanol, dried under a N_2 stream and dried sufficiently on a hot plate at a constant temperature of 80 ^{0}C prior to the synthesis. The FTO substrates were placed into an autoclave containing thoroughly mixed 1:1 solutions of hydrochloric acid, deionized water (30 ml), and 0.3 mL titanium (IV) butoxide. Autoclave was maintained at 150 ^{0}C for 6 h. After the synthesis, samples were thoroughly washed by deionized water and dried under nitrogen flow. Crystallinity of nanorods was improved by annealing in air at 450 ^{0}C for 4 h.

Preparation of Cobalt oxide/TiO_2 Nanorod on FTO

Cobalt nanoparticles on TiO_2 nanorods were deposited electrochemically using a conventional three electrode system at a constant voltage of -0.5 V for various time period (20, 40, 60 seconds) with an aqueous solution of $CoCl_2.6H_2O$ (0.01 M) purged with N_2 gas for 1 hour prior to the experiment. TiO_2 nanorod/FTO, Ag/AgCl (saturated with KCl), and Pt mesh were used as working electrode, reference electrode, and counter electrode respectively. The as-deposited substrates were converted to Cobalt oxide by oxidizing thermally at various temperatures (350, 375, 400, 500, 600^{0}Cand 700^{0}C) using a Rapid Thermal Annealing (RTA, ULVAC RIKO INC, MILA-3000) apparatus with a heating and cooling rate of

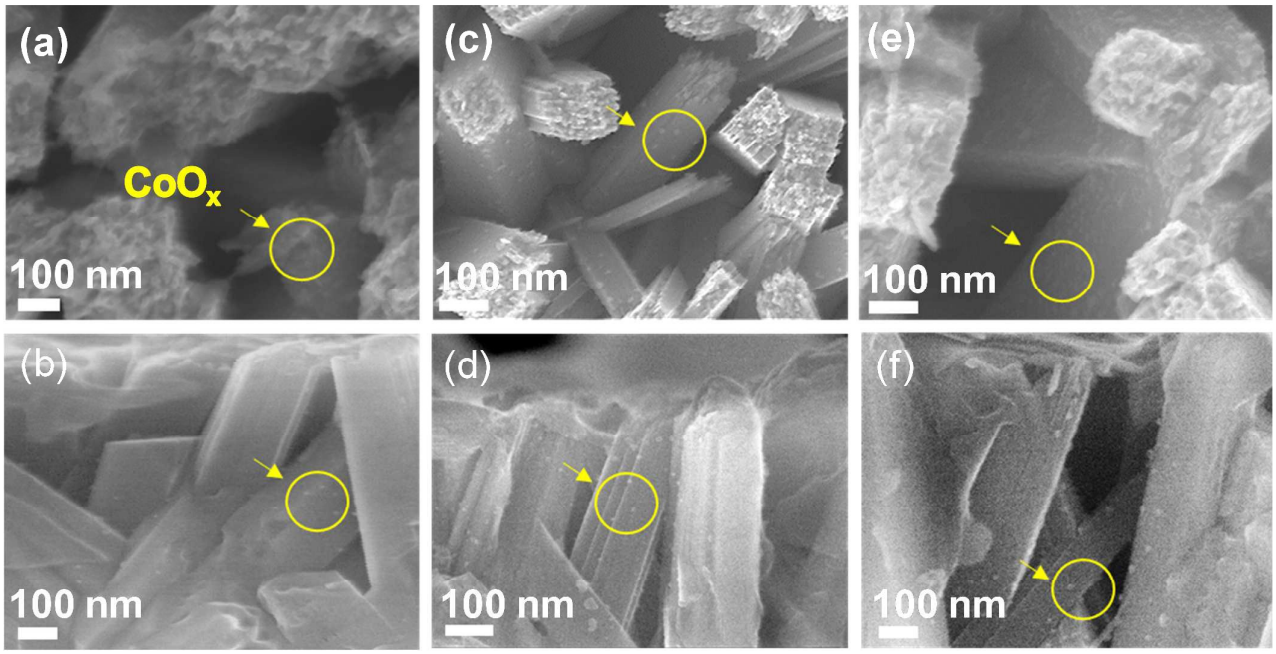

Figure 2. Horizontal and vertical SEM image of the Cobalt oxide nanoparticle on TiO_2 nanorod/FTO with varying electrodeposition time of (a) and (b) 20 second, (c) and (d) 40 second, (e) and (f) 60 seconds, annealing at 500^0C in air.

10^0C/second and holding the sample at respective temperature for 600 seconds with nitrogen gas flown at a rate of 0.01 L/min. As a result, hetero-junction electrodes of Cobalt oxide/TiO_2/FTO were obtained.

The morphology and microstructural characterizations of the nanostructured samples were performed using a field emission scanning electron microscope (FE-SEM, JSM-6500 F, JEOL), a field emission transmission electron microscope (FETEM, 200kV/JEM-ARM200F, JEOL), and an X-ray diffractometer (XRD, SWXD, Rigaku). EELS spectra were taken in a STEM (JEM-ARM200F, JEOL) at 200 kV with a spherical aberration (Cs) corrector and Gatan image filter (GIF Quantum ER, Gatan). Electrochemical measurements were carried out using a potentiostat (AMT VERSASTAT 3, Princeton Applied Research) with a three electrode configuration consisting of a platinum (Pt) wire counter electrode and a saturated Ag/AgCl reference electrode in 0.1 M Na_2S (pH ~ 12.5) electrolyte. A working electrode with a 1 cm^2 area was illuminated using a 1 kW xenon lamp (Newport) with its infrared wavelengths filtered out by water, and wavelengths below 420 nm removed by an optical filter, enabling measurements under visible light. The light irradiance, measured by a thermopile detector, was 100 mW/cm^2.

Results and discussion

Formation of nanostructure and effect of electrodeposition time

The top view of SEM images (Figure 1a, c, and e) shows the images of TiO_2 nanorods on FTO after Cobalt oxide nanoparticle deposition. The as-deposited Cobalt oxide nanoparticles (5 ~ 15 nm) on densely grown TiO_2 nanorods having a length of between 1~ 2 µm, can be clearly seen from the vertical images shown in figure 1b, d, and f. There is a linear relationship between electrodeposition time and size of Cobalt oxide nanoparticle which will be discussed in detail by coupling with TEM results. The deposition of Cobalt oxide nanoparticles on TiO_2 nanorod was further confirmed by EDS analysis (supporting information figure SI 1b). The characteristics and basic properties of rutile nanorods were described elsewhere previously by our research group.[32, 35]

Chemical and crystal structures were further confirmed by XRD analysis. To get a clear cut idea

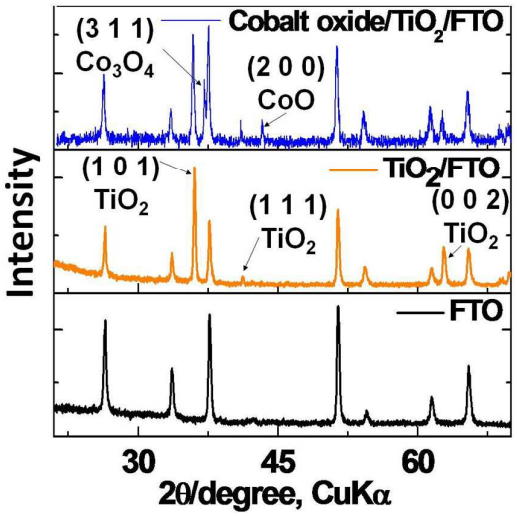

Figure 3. Comparison of XRD peaks of FTO substrate, TiO_2 nanorod on FTO and Cobalt oxide on TiO_2 nanorod/FTO annealed at 500^0C in air.

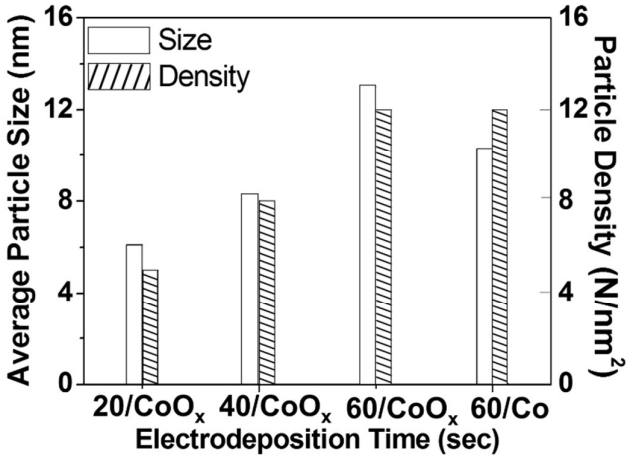

Figure 4. Relation between particle size and particle density with respect to electrodeposition time of Cobalt and its oxide formed on TiO_2 nanorod with and without annealing at 500^0C in air.

about the characteristic peaks of Cobalt oxide (JCPDS#01-070-2855, JCPDS#01-074-1656), the peaks due to TiO_2 nanorods and FTO were shown in figure 3 (JCPDS#01-070-7347). XRD analysis of TiO_2 nanorods shown in Figure 3 reveals that the nanorods are single crystalline with tetragonal rutile structure growing dominantly in the (002) direction. In XRD analysis diffraction peak of TiO2 (002) is prominent among diffraction peaks corresponding to TiO_2. From figure 3 we can clearly see that Cobalt deposited was oxidised with the formation of both CoO and Co_3O_4 (electrodeposition for 60 seconds, at -0.5 V, annealed at 500^0C in air). (200) and (311) planes in the XRD pattern is assigned to the cubic phase of CoO and Co_3O_4. The formation of Cobalt oxide in mixture is quite expected in our system as annealing temperature is below 1000^0C. Above 1000^0C, all oxides of Cobalt will be converted to CoO.

TEM analysis of Cobalt oxide nanoparticles on TiO_2 nanorod which were electrodeposited as a function of time was carried out (supporting information Figure SI 3) with the same condition as that of SEM analysis. Nanoparticle anchoring on nanorods is quite obvious from the Figure 2. Size of nanoparticles was found to be varying between 5 to 15 nm in diameter. SAED patterns of both Cobalt oxide and TiO_2 nanoparticles were determined, (220) and (200) planes correspondi-

ng to Co_3O_4 and CoO respectively. Existence of (100) and (200) planes corresponding to TiO_2 were observed. From the lattice-fringe analysis, shown in Figure SI 3, {(220) – Co_3O_4, (200) – further confirmed the presence CoO and Co_3O_4 formation. By comparing with standard data (JCPDS#01-070-2855, JCPDS#01-074-1656), nanoparticles formed on the nanorods of TiO_2 were further confirmed to be mixture of both CoO and Co_3O_4.

As described earlier, both SEM and TEM analysis clearly showed that electrodeposition time was found to have crucial role in the size of Cobalt oxide nanoparticle.Particle size of Cobalt oxide irrespective of the nature of oxide was averaged and shown in Figure 4 schematically. Detailed information is shown in supporting information (Figure SI 3). We can see that there is a linear relation between electrodeposition time and particle size. As it is expected when oxidized, average size of the particle was also found to be increased. The linearity in relationship of electrodeposition time was found to be applicable for Cobalt oxide nanoparticle density as well (Figure 4). Particle density was calculated over a specific area for nanoparticle anchored on TiO_2 nanorod (200 x 200 nm^2). Nanoparticle size and density have got significant importance in photocatalytic semiconductor systems. It is reported that band gap of Cobalt oxide has a large on particle size. Bao et. al, shown that microcrystalline

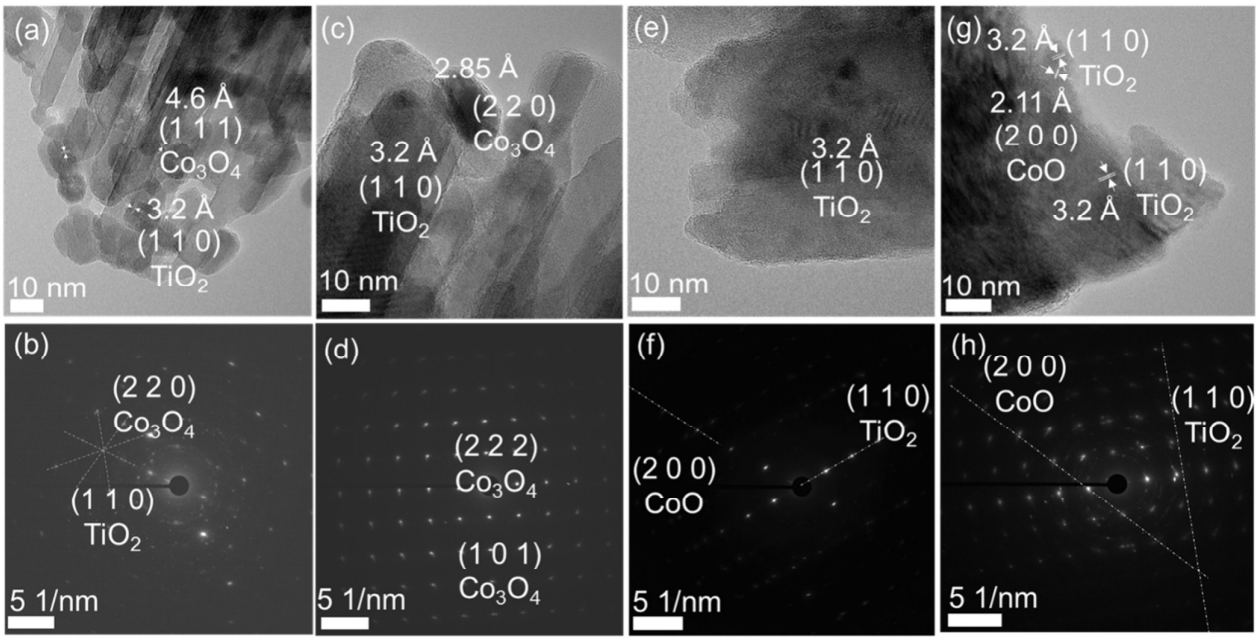

Figure 5. Lattice-fringe TEM images and SAED patterns of Cobalt oxides nanoparticles on TiO_2 nanorod with annealing temperature of 700^{0}C (a - d) and 350^{0}C (e - h) in air (a, b, e, and f) and nitrogen (c, d, g, and h).

CoO can be potentially made active for overall water splitting just by changing the particle size. The band position was shifted ~1.5 eV with band gap remaining to be almost same (2.6 eV). In our system it may not have crucial influence in photocatalytic activity as we use p-n hetero-junction system which already cause a fermi level alignment leading to shift in band positions.[25]

Effect of annealing temperature and ambient

More importantly, we then investigated the effect of annealing temperature and atmosphere on the oxide formation of Cobalt. Figure 5 shows the detailed analysis. At this time, voltage (-0.5 V), electrodeposition time (40 seconds), and annealing time in RTA (10 minute) were kept constant. Nanoparticle formations of Cobalt oxide on TiO_2 nanorod can be evidently seen from Figure 5 (a), (c), (e), and (g). From SAED patterns and lattice-fringe images, the formation and nature of Cobalt oxide nanoparticles were determined and summarized in Table 1. We have also elucidated the microstructure of sample annealed in air and nitrogen atmosphere (Figure SI 4, 5, 6 and 7). Very interestingly, we have found the limiting condition for the selective formation of Cobalt oxide depending on annealing temperature and atmosphere. Annealing at 700^{0}C and 350^{0}C showed monotonic oxide formation of Co_3O_4 and CoO respectively. In addition, mixture of Cobalt oxide formed at 600^{0}C in nitrogen was changed to Co_3O_4 alone when annealed in air. Similarly CoO single-handedly formed at 375^{0}C when annealed under nitrogen atmosphere. All other intermediate temperature annealing gave rise to mixture of oxides

Table 1. Effect of annealing temperatures and medium on Cobalt oxide formation from electrodeposited Co/TiO_2 nanorod, presence and absence marked by "✓" and "X"respectively.

RTA	CoO		Co_3O_4	
	Air	N_2	Air	N_2
350^{0}C			X	X
375^{0}C				X
400^{0}C				
500^{0}C				
600^{0}C	X			
700^{0}C	X	X		

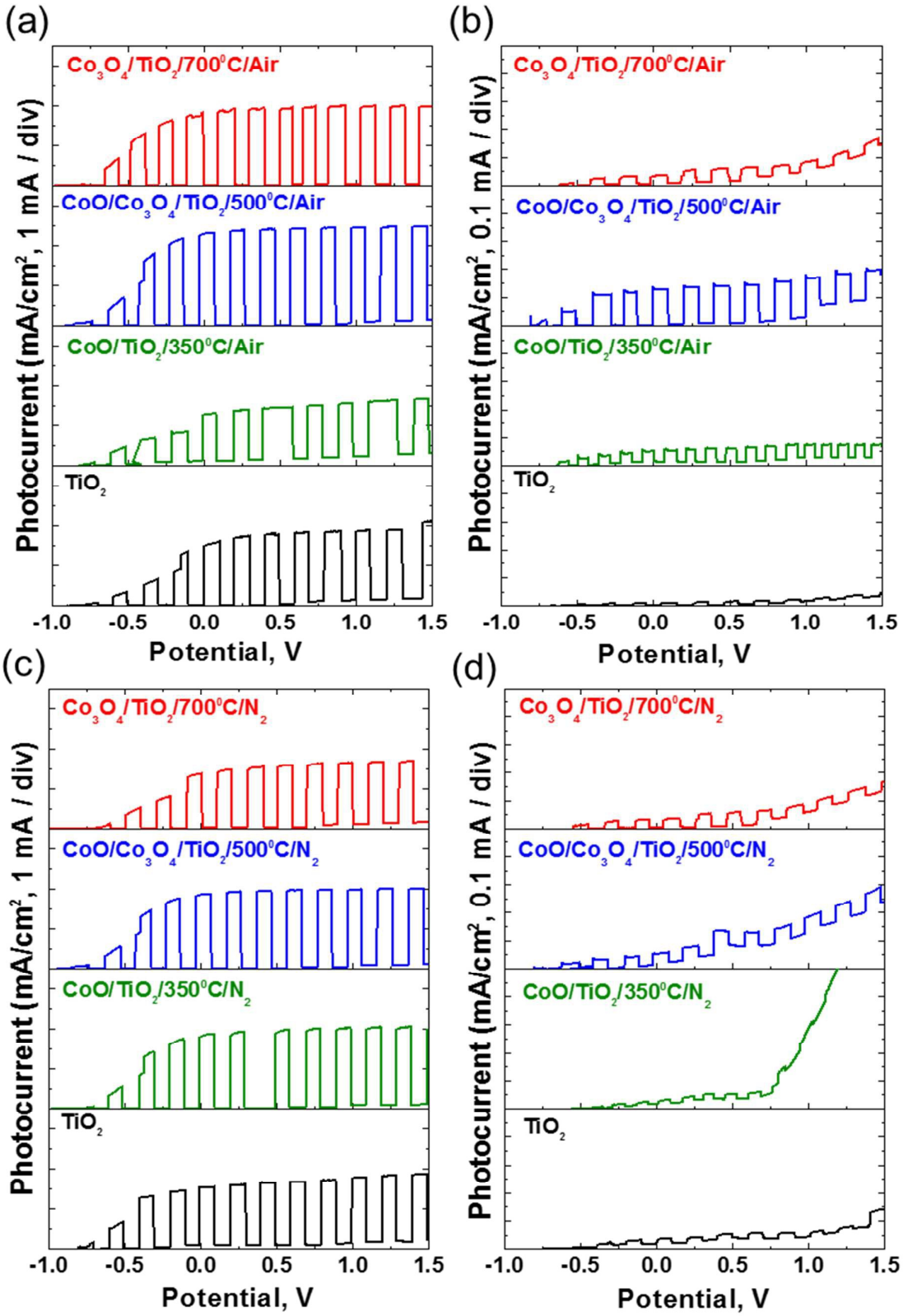

Figure 6. Comparison of white and visible light photocurrent density-voltage diagram of Cobalt oxide/TiO_2 nano structure and TiO_2 nanorod on FTO in 0.1 M Na_2S aqueous solution with light intensity 100 mW/cm^{-2} annealed in (a), (b) air and (c), (d) in N_2 respectively.

irrespective of the annealed atmosphere.

irrespective of the annealed atmosphere.

The formation of mixture of Cobalt oxide nanoparticles on TiO_2 nanostructure was further confirmed by EELS spectra (supporting information SI 2). Cobalt oxide was characterized by the shape and position of O-K edge at 532 eV and Co-L at 779 eV.[36] The data obtained in EELS was very well matched to the TEM results. In the case of sample annealed at 500^0C, mixtures of oxides of Cobalt were formed. This was confirmed by splitting of peak at 532 into two, which is a characteristic of Co_3O_4. The peak at 565 corresponds to Cobalt monoxide. In addition, the ratio of intensity of Co-L peaks (L_2 and L_3) showed the presence of mixture of oxides having the values of ~4.9 and ~2.9 which correspond to CoO and Co_3O_4 respectively. At the same time, sample prepared at 600^0C annealed in air was found to be containing monotonic L_2/L_3 intensity ratio of ~3.0 corresponding to Co_3O_4.

Comparative study of photoelectrochemical properties

Photocurrent densities of the as-prepared Cobalt oxide/TiO_2 nanostructure were measured in each condition which was prepared as a function of electrodeposition time, annealing temperature, atmosphere (air and N_2), and concentration of electrolyte used for electrodeposition (Figure 6, SI Figure 11, and SI Figure 12). Both white light and visible light were used as the light source. Prior to the sensitization with the Cobalt oxide, photocurrent density of the bare TiO_2 was also measured for comparison. Under white and visible light the photocurrent density was found to be enhanced after sensitization at zero voltage. This can be easily read out from the Figure 6. The enhancement in the photocurrent shows the effective sensitization of Cobalt oxide and titanium dioxide. Both in the case of air and N_2 annealed condition, sample with mixture of oxides (CoO and Co_3O_4) showed maximum photocurrent enhancement (15 times under visible light irradiation).The obvious reason could be the band gap of Co_3O_4 and CoO which is in between 2.1 to 2.6 eV (470 to 590 nm). In addition, samples with lower electrodeposition time (smaller nanoparticle size) lead increased photocatalytic activity.

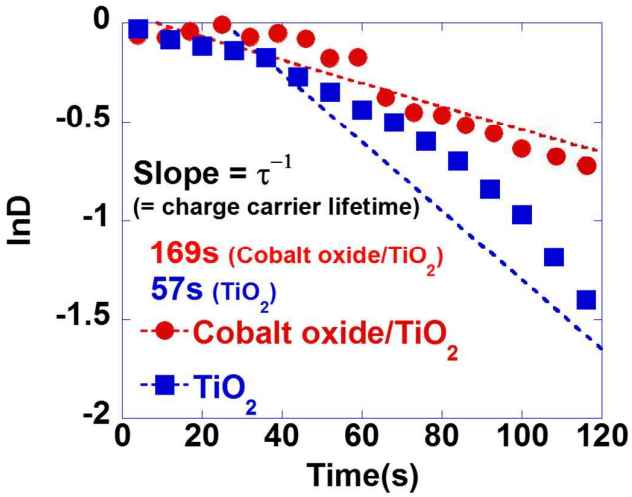

Figure 7. Photocurrent density kinetics of Cobalt oxide/TiO_2/FTO and TiO_2/FTO with biased (V_B = 0.5 V vs Ag/AgCl) electrodes in 0.1 M Na_2S (pH = 12. 5) solution under white light irradiation (100 mW/cm^2)

In addition, we have also tried to investigate the effect of concentration of electrodeposition solution on photocatalytic activity. We found that lowering the concentration of electrodeposited solution resulted in improved PEC properties. We varied the concentration from 60 mM to 4 mM. This clearly shows that amount of the nanoparticle formed on nanostructure has a saturation limit. Large amount of nanoparticles lead to decrease in photocurrent with poor p-n junction formation plausibly due to steric factor.

A schematic representation of the hetero-junction formed in our case is depicted in Figure 1c. Since we anchored the nanoparticles of Cobalt oxide on TiO_2, both were in contact with electrolyte solution and upon light irradiation electron-hole pair will be formed in both semiconductors. As previously described photogenerated electron will move from the conduction band of Cobalt oxide to that of TiO_2 and then to FTO substrate finally reaching the metallic counter electrode and hole movement in the reverse direction. Direct evidence for the formation of a effective hetero-junction is shown in Figure 7. Transient times of the TiO_2 nanorods with and without Cobalt oxide nanoparticles were measured to comparatively investigate the recombination rates. Transient changes in the photocurrents as a function of elapsed time were

measured by irradiating pulsed light (on and off). Charge carrier lifetime were calculated by relating the following standard equations:[32]

$$D = [I(t) - I(f)]/ [I(i) - I(f)] \quad (1)$$

$$D = \exp(-t/\tau) \quad (2)$$

where t is a time, D denotes defining parameter for photocurrent relaxation, τ is the recombination time, I (i) and I (f) are initial final value of photocurrent and I (t) is the time duration with pulsed light. Transient time constant (τ) is obtained from the inverse slope plotted between In(D) and time as shown in Figure 7. Transient times of hetero-system were found to be 3 times larger than bare TiO_2 nanorod signifying improved PEC properties.

Conclusions

Cobalt oxide nanoparticles were anchored on TiO_2 nanorods with different conditions so as to improve the photocatalytic properties. Size of the nanoparticles was found to increase with increase in electrodeposition time. Cobalt oxides (CoO/Co_3O_4) were formed selectively with respect to RTA temperatures and ambient (oxygen partial pressure). Higher temperature (700^0C) favoured the more stable Co_3O_4 oxidation state of Cobalt. With lowering of temperature, monoxide was also formed leading to the state of mixed oxides and finally CoO solely formed at 350^0C. Photocurrent under visible and white light showed maximum improvement when CoO and Co_3O_4 co-existed together. Charge carrier measurement further evidenced the formation of improved hetero-system formed between Cobalt oxide and TiO_2 nanorods. Most importantly, here we have demonstrated a simple, low cost and two-step process to synthesize metal oxide nanoparticle by electrodeposition even on a dense nanostructured substrate.

Acknowledgements

This work was supported by the National Research Fou ndation of Korea(NRF) grant funded by the Korea gover nment (MSIP) (No.2014R1A2A2A01005324).

Notes and References

[a]*School of Advanced Materials and System Engineering, Kumoh National of Institute of Technology,Yangho-dong, Gumi-si, Gyeongsangbuk-do, Korea E-mail: blyang@kumoh.ac.kr*
[b]*Electronics& Information Technology Research Institute Gumi, 17 Chomdangieop 1 St. Sandong, Gumi, Gyeongbuk, Korea. 730-853.*

† Electronic supplementary information (ESI) available:

1. T. Lopes, P. Dias, L. Andrade and A. Mendes, *Solar Energy Materials and Solar Cells*, 2014, **128**, 399-410.
2. K. Maeda and K. Domen, *The Journal of Physical Chemistry Letters*, 2010, **1**, 2655-2661.
3. L. J. Minggu, W. R. W. Daud and M. B. Kassim, *International Journal of Hydrogen Energy*, 2010, **35**, 5233-5244.
4. H. M. Chen, C. K. Chen, R.-S. Liu, L. Zhang, J. Zhang and D. P. Wilkinson, *Chemical Society Reviews*, 2012, **41**, 5654-5671.
5. T. Hisatomi, J. Kubota and K. Domen, *Chemical Society Reviews*, 2014, **43**, 7520-7535.
6. A. A. Ismail and D. W. Bahnemann, *Solar Energy Materials and Solar Cells*, 2014, **128**, 85-101.
7. J. Jasieniak, M. Califano and S. E. Watkins, *ACS nano*, 2011, **5**, 5888-5902.
8. A. Kudo and Y. Miseki, *Chemical Society Reviews*, 2009, **38**, 253-278.
9. H. Xia, C. Hong, B. Li, B. Zhao, Z. Lin, M. Zheng, S. V. Savilov and S. M. Aldoshin, *Advanced Functional Materials*, 2015, **25**, 627-635.
10.S. J. Moniz, S. A. Shevlin, D. J. Martin, Z.-X. Guo and J. Tang, *Energy & Environmental Science*, 2015, **8**, 731-759.
11.A. J. Nozik, *Nano letters*, 2010, **10**, 2735-2741.
12.F. E. Osterloh, *Chemical Society Reviews*, 2013, **42**, 2294-2320.
13.J. Ran, J. Zhang, J. Yu, M. Jaroniec and S. Z. Qiao, *Chemical Society Reviews*, 2014, **43**, 7787-7812.
14.R. Vogel, P. Hoyer and H. Weller, *The Journal of Physical Chemistry*, 1994, **98**, 3183-3188.
15.L. Wang, J. Ge, A. Wang, M. Deng, X. Wang, S. Bai, R. Li, J. Jiang, Q. Zhang and Y. Luo, *Angewandte Chemie International Edition*, 2014, **53**, 5107-5111.
16.L. Dlamini, R. Krause, G. Kulkarni and S. Durbach, *Mater. Chem. Phys.*, 2011, **129**, 406-410.

17.Z. Li, X. Cui, H. Hao, M. Lu and Y. Lin, *Materials Research Bulletin*, 2015, **66**, 9-15.
18.Y. Ma, X. Wang, Y. Jia, X. Chen, H. Han and C. Li, *Chem. Rev.*, 2014, **114**, 9987-10043.
19.M. Paulose, K. Shankar, S. Yoriya, H. E. Prakasam, O. K. Varghese, G. K. Mor, T. A. Latempa, A. Fitzgerald and C. A. Grimes, *The Journal of Physical Chemistry B*, 2006, **110**, 16179-16184.
20.Y.-C. Pu, G. Wang, K.-D. Chang, Y. Ling, Y.-K. Lin, B. C. Fitzmorris, C.-M. Liu, X. Lu, Y. Tong and J. Z. Zhang, *Nano letters*, 2013, **13**, 3817-3823.
21.C. Ruan, M. Paulose, O. K. Varghese, G. K. Mor and C. A. Grimes, *The Journal of Physical Chemistry B*, 2005, **109**, 15754-15759.
22.Q. Jin, H. Yamamoto, K. Yamamoto, M. Fujishima and H. Tada, *Phys. Chem. Chem. Phys.*, 2013, **15**, 20313-20319.
23.L. Liao, Q. Zhang, Z. Su, Z. Zhao, Y. Wang, Y. Li, X. Lu, D. Wei, G. Feng and Q. Yu, *Nature nanotechnology*, 2014, **9**, 69-73.
24.Y.-Q. Mao, Z.-J. Zhou, T. Ling and X.-W. Du, *RSC Advances*, 2013, **3**, 1217-1221.
25.Y. Qin, G. Wang and Y. Wang, *Catalysis Communications*, 2007, **8**, 926-930.
26.Y.-F. Wang, M.-C. Hsieh, J.-F. Lee and C.-M. Yang, *Applied Catalysis B: Environmental*, 2013, **142**, 626-632.
27.G. Zhang, H. Huang, W. Li, F. Yu, H. Wu and L. Zhou, *Electrochimica Acta*, 2012, **81**, 117-122.
28.L. Zhang, Z. Gao, C. Liu, Y. Zhang, Z. Tu, X. Yang, F. Yang, Z. Wen, L. Zhu and R. Liu, *Journal of Materials Chemistry A*, 2015, **3**, 2794-2801.
29.X. Zheng, G. Shen, Y. Li, H. Duan, X. Yang, S. Huang, H. Wang, C. Wang, Z. Deng and B.-L. Su, *Journal of Materials Chemistry A*, 2013, **1**, 1394-1400.
30.E. A. Gulbransen and K. F. Andrew, *Journal of the Electrochemical Society*, 1951, **98**, 241-251.
31.Y. Fan, N. Zhang, L. Zhang, H. Shao, J. Wang, J. Zhang and C. Cao, *Electrochimica Acta*, 2013, **94**, 285-293.
32.H. Kim and B. L. Yang, *International Journal of Hydrogen Energy*, 2015, **40**, 5807-5814.
33.U. Shaislamov, H. Kim and B. L. Yang, *Journal of Materials Research*, 2013, **28**, 497-501.
34.U. Shaislamov and B. L. Yang, *Journal of Materials Research*, 2013, **28**, 418-423.
35.U. Shaislamov and B. L. Yang, *International Journal of Hydrogen Energy*, 2013, **38**, 14180-14188.
36.D. Barreca, A. Gasparotto, O. I. Lebedev, C. Maccato, A. Pozza, E. Tondello, S. Turner and G. Van Tendeloo, *CrystEngComm*, 2010, **12**, 2185-2197.

Table of content – Graphical Abstract

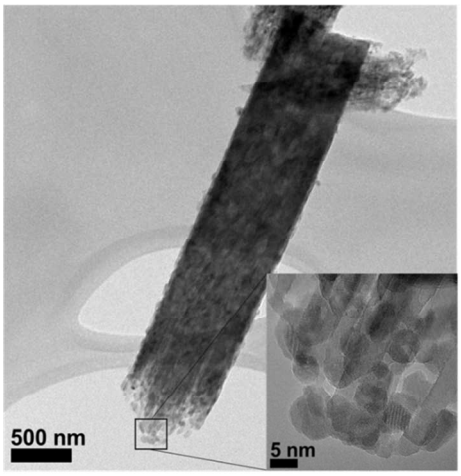

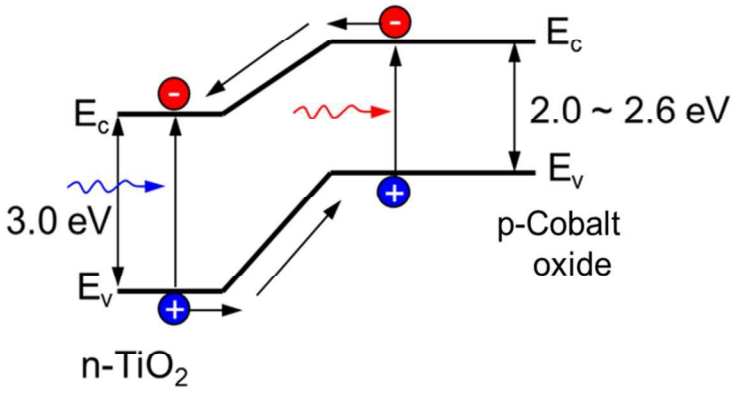

Simple, low cost, two-step synthesis of Cobalt oxide nanoparticle sensitized on TiO_2 nanorods with enhanced photoelectrochemical properties.